SCIENCE CHINA
Information Sciences

• RESEARCH PAPER •

August 2018, Vol. 61 082305:1–082305:14
https://doi.org/10.1007/s11432-017-9278-0

Uplink spectral efficiency analysis of multi-cell multi-user massive MIMO over correlated Ricean channel

Juan CAO[1,2*], Dongming WANG[2], Jiamin LI[2], Qiang SUN[1,2] & Ying HU[3]

[1]*School of Electronics and Information, Nantong University, Nantong* 226019*, China;*
[2]*National Mobile Communications Research Laboratory, Southeast University, Nanjing* 210096*, China;*
[3]*School of Electronics and Information, Jiangsu University of Science and Technology, Zhenjiang* 212003*, China*

Received 2 June 2017/Revised 28 July 2017/Accepted 10 October 2017/Published online 18 May 2018

Abstract In this study, the performance of uplink spectral efficiency in massive multiple input multiple output (MIMO) over a spatially correlated Ricean fading channel is presented. The maximum ratio combining (MRC) receiver is employed at the base station (BS) for two channel estimation methods. The first method is based on pilot-assisted least minimum mean square error (LMMSE) estimation, whereas the second is based on line-of-sight (LOS). The respective analytical expressions of the uplink data rate are given for these two methods. Because of the existence of pilot contamination, the uplink data rate of the pilot-assisted LMMSE estimation method approaches a finite value (we call it the asymptotic rate in this study) when the BS antenna number is high. However, the data rate of the LOS method is linear with the number of BS antennas. The expression of the uplink rate of the LOS method also shows that for a Ricean channel, the spatial correlation between the BS antennas may either decrease the rate or increase the rate, depending on user location. This conclusion explains why the spatial correlation may increase rather than decrease the data rate of pilot-assisted LMMSE. We also discuss the power scaling law of the two methods, and show that the asymptotic expressions of the two methods are the same and both are independent of the antenna correlation.

Keywords massive MIMO, pilot contamination, Ricean fading, spacial correlation, uplink rate

Citation Cao J, Wang D M, Li J M, et al. Uplink spectral efficiency analysis of multi-cell multi-user massive MIMO over correlated Ricean channel. Sci China Inf Sci, 2018, 61(8): 082305, https://doi.org/10.1007/s11432-017-9278-0

1 Introduction

Massive multiple input multiple output (MIMO) technology has been investigated for its remarkable potential to increase spectral and energy efficiency even with a very simple linear transmitter/receiver [1–4]. However, increasing the number of antennas leads to new challenges such as obtaining accurate channel state information (CSI). For time division duplexing (TDD) systems, the downlink CSI can be obtained by using uplink pilots and exploiting channel reciprocity. However, estimation errors, feedback delay and quantized errors will occur, which impair system performance. In addition, since the coherence time is limited, the number of orthogonal pilots is restricted. So we have to reuse the same pilot sequences in different cells, which causes pilot contamination. The system capacity of massive MIMO is hardly

* Corresponding author (email: cj@ntu.edu.cn)

determined by the reuse of pilot sequences between the nearby cells [5]. Reducing the pilot contamination is crucial to further improving massive MIMO performances.

Ref. [6] proposed a new multi-cell minimum mean square error (MMSE)-based precoding method in order to reduce pilot contamination. For the TDD system, the overall cells are divided into two groups, where the users in the cells of one group transmit pilot sequence to base stations (BSs), whereas users in cells of the other group receive data. Through this arrangement, pilot contamination remains only within the same group and is efficiently reduced without inter-cell cooperation [7, 8]. In such technologies, the signal to interference plus noise ratio (SINR) of user is limited and cannot reach infinity with an increase in the number of BS antennas. However, effects of pilot contamination are related to the pilot assignment scheme. As a result, many researchers have studied how to optimize the pilot assignment or scheduling schemes [9–12]. In addition, some studies have indicated that pilot contamination is not inevitable. For example, in the event that covariance matrices satisfy a certain non-overlapping condition on their dominant subspaces, a Bayesian channel estimation method that explicitly uses covariance information can completely remove pilot contamination effects [13]. Because the source of pilot contamination lies in using pilot-assisted channel estimation, the channel can be estimated blindly. Then, the pilot contamination is avoided because no pilots are used [14–16]. Considering the inherent sparsity of wireless channel, we can employ sparsity channel estimation and pilot design using compressive sensing technology to reduce pilot overhead and pilot contamination [17–19].

The other challenge of massive MIMO lies in the limited space at the BS-side, which creates difficulties in antenna mounting. In addition, millimeter-wave (mm-wave) wireless systems are emerging as a promising technology for full exploitation of a spatial multiplex and development of a higher spectrum. The millimeter-wave operates from 30 to 300 GHz with a wavelength between 1 to 10 mm, and the smaller wavelength enables a large number of antennas to be mounted in the limited space [20, 21]. Because of the highly directional nature of propagation, line-of-sight (LOS) propagation plays an important role in mm-wave. In addition, when the cell coverage is shrunk, the channel between users and the BS will likely include the LOS component [22, 23]. As a result, the LOS is expected to be a new propagation mode for massive MIMO. However, the majority of studies are based on the assumption of the Rayleigh fading model, which simplifies the mathematic model and analysis. The Rayleigh model is no longer suitable when an LOS exists. The Ricean fading model is applicable when the wireless link between the transmitter and receiver has an LOS component in addition to the diffused Rayleigh component. Ref. [24] investigated the uplink rate of massive MIMO over iid Ricean fading channels.

In this study, we investigate the uplink data rate of massive MIMO over correlated Ricean fading channels for two CSI estimation methods. The first method is a maximum ratio combining (MRC) based on pilot-assisted least minimum mean square error (LMMSE) estimation, which causes pilot contamination. In order to avoid pilot contamination, similar to [25], we take the first order statistical information as the estimated channel. This means using the LOS component as the estimated channel, while the diffused component is regarded as interference. The main contributions of this study are as follows.

(1) We deduce the respective analytical expressions for two methods. Because of the existence of pilot contamination, the uplink data rate of the pilot-assisted LMMSE estimation method approaches a finite value when the number of BS antennas is very high. However, the infinite uplink achievable rate of the LOS method is linear with the number of BS antennas. This means that as the number of BS antennas increases, the gap between the two methods will become increasingly smaller, and finally the rate of LOS method will exceed that of the pilot-assisted LMMSE estimation method.

(2) The effect of Ricean fading on the uplink data rate has been investigated extensively. Based on the expression of the achievable rate of the LOS method, we find that the correlation between the BS antennas may either decrease or increase the rate depending on user location. Therefore, if the locations of users cause antenna correlation to increase the rate with an increase of the Ricean factor, the rate of the pilot-assisted LMMSE estimation method will become larger as a result of antenna correlation, because the effect of the LOS component becomes stronger.

(3) We also discuss the power scaling law of the two methods. When the number of base station antennas is very high, the asymptotical expressions of the two methods are the same and both are

independent of the antenna correlation.

2 System model

Consider the L cells system with one BS and K mobile users in each cell. Each BS is equipped with N antennas, and each user has a single antenna. We assume that the system is operating on TDD protocol with full frequency reuse. Taking cell 1 as the reference cell, the uplink received base-band signal vector is given by

$$\boldsymbol{y} = \sqrt{p_{\mathrm{u}}}\boldsymbol{G}_1\boldsymbol{x}_1 + \sqrt{p_{\mathrm{u}}}\sum_{l=2}^{L}\boldsymbol{G}_l\boldsymbol{x}_l + \boldsymbol{w}, \tag{1}$$

where $\boldsymbol{y} = [y_1 \cdots y_N]^{\mathrm{T}}$ is the received signal vector, $\boldsymbol{x}_l = [x_{l,1} \cdots x_{l,K}]^{\mathrm{T}} \sim \mathcal{CN}(\boldsymbol{0}, \boldsymbol{I}_K)$, where $x_{l,k}$ is the transmitted signal of user k in the lth cell, and p_{u} is the average transmit power of each user. $\boldsymbol{G}_l = [\boldsymbol{g}_{l,1} \cdots \boldsymbol{g}_{l,K}]$ is the composite channel matrix of all K users in the lth cell to the reference cell. $\boldsymbol{w}$ is the additive noise vector that satisfies standard complex Gaussian distribution. Because the distance between the users in the reference cell and the reference BS is small, the channel of users in the reference cell is modeled so that it consists of two parts: a deterministic component corresponding to the LOS path and a Rayleigh-distributed random component that accounts for the scattered signals. By contrast, the distance between users in the interfering cell and the reference BS is large. Therefore, the LOS component is no longer present in channels because of the scatters and building blocks. Based on this, the fast fading can be modeled as

$$\boldsymbol{H}_l = \begin{cases} \bar{\boldsymbol{H}}_1\left[\boldsymbol{\Omega}(\boldsymbol{\Omega}+\boldsymbol{I}_K)^{-1}\right]^{\frac{1}{2}} + \widehat{\boldsymbol{H}}_1\left[(\boldsymbol{\Omega}+\boldsymbol{I}_K)^{-1}\right]^{\frac{1}{2}}, & l=1, \\ \widehat{\boldsymbol{H}}_l, & l\neq 1, \end{cases} \tag{2}$$

where $[\bar{\boldsymbol{H}}_1]_{N\times K}$ is the deterministic component with $[\bar{\boldsymbol{H}}_1]_{n,k} = \mathrm{e}^{-\mathrm{j}(n-1)\frac{2\pi d}{\lambda}\sin\theta_k}$, d is the antenna spacing, λ is the wavelength, and $\theta_k \sim [-\pi/2, \pi/2]$ is the arrival angle of the kth user in the reference cell. $[\widehat{\boldsymbol{H}}_l]_{N\times K} = [\boldsymbol{h}_{l,1}\boldsymbol{h}_{l,2}\cdots\boldsymbol{h}_{l,K}]$ denotes the channel matrix for fast fading between the users in each cell and the reference BS that satisfies the standard complex Gaussian distribution. $\boldsymbol{\Omega}$ is a diagonal matrix with $\boldsymbol{\Omega}_{k,k} = \vartheta_k$ as the kth element denoting the Ricean factor that represents the ratio of the power of the deterministic component to that of the fading component. The bigger ϑ_k is, the more deterministic is the channel. Considering the correlation between the BS antennas and assuming all user correlations are the same, the composite channel matrix can be expressed as

$$\boldsymbol{G}_l = \begin{cases} \bar{\boldsymbol{G}}_1\left[\boldsymbol{\Omega}(\boldsymbol{\Omega}+\boldsymbol{I}_K)^{-1}\right]^{\frac{1}{2}} + \widehat{\boldsymbol{G}}_1\left[(\boldsymbol{\Omega}+\boldsymbol{I}_K)^{-1}\right]^{\frac{1}{2}}, & l=1 \\ \widehat{\boldsymbol{G}}_l, & l\neq 1 \end{cases} \tag{3}$$

where

$$\bar{\boldsymbol{G}}_1 = [\bar{\boldsymbol{g}}_{1,1}\cdots\bar{\boldsymbol{g}}_{1,K}] = \bar{\boldsymbol{H}}_1\boldsymbol{\Lambda}_1^{\frac{1}{2}},$$
$$\widehat{\boldsymbol{G}}_l = \left[\widehat{\boldsymbol{g}}_{l,1}\cdots\widehat{\boldsymbol{g}}_{l,K}\right] = \boldsymbol{R}^{\frac{1}{2}}\widehat{\boldsymbol{H}}_l\boldsymbol{\Lambda}_l^{\frac{1}{2}},$$

$\boldsymbol{\Lambda}_l = \mathrm{diag}(\,\lambda_{l,1}\ \cdots\ \lambda_{l,K}\,)$ with $\lambda_{l,k}$ representing the slow fading (including the shadow and path loss), and $\boldsymbol{R}$ is the deterministic receive correlation matrix. $\boldsymbol{R}$ has the following properties: positive definite, $\mathrm{Tr}\,[\boldsymbol{R}] = N$, and having uniformly bounded spectral norm.

3 Uplink rate analysis using pilot-assisted LMMSE channel estimate

3.1 LMMSE channel estimate

Assuming that both the deterministic LOS component and the Ricean factor matrix $\boldsymbol{\Omega}$ are perfectly known at both the transmitter and receiver, only the Rayleigh fading part needs to be estimated. We

define the estimated channel matrix as

$$\hat{\boldsymbol{G}}_l = \begin{cases} \bar{\boldsymbol{G}}_1 \left[\boldsymbol{\Omega}(\boldsymbol{\Omega}+\boldsymbol{I}_K)^{-1}\right]^{\frac{1}{2}} + \hat{\widehat{\boldsymbol{G}}}_1 \left[(\boldsymbol{\Omega}+\boldsymbol{I}_K)^{-1}\right]^{\frac{1}{2}}, & l=1, \\ \hat{\widehat{\boldsymbol{G}}}_l, & l \neq 1. \end{cases} \tag{4}$$

In the multi-cell scenario, non-orthogonal training sequences must be used because the orthogonal pilot resources are limited as a result of the coherence time of the channel. During the uplink pilot transmission, users in all cells simultaneously transmit the pilot sequence of length τ. In addition, $K \leqslant \tau < T$, where T is the coherence time of the channel. We let $\tau = K$. Therefore, the training matrix is a $K \times K$ unitary matrix that satisfies $\boldsymbol{\Phi}^{\mathrm{H}}\boldsymbol{\Phi} = \boldsymbol{I}_K$. The received pilot signals at the reference cell can be expressed as

$$\boldsymbol{Y}_{\mathrm{P}} = \sqrt{p_{\mathrm{P}}} \left\{ \bar{\boldsymbol{G}}_1 \left[\boldsymbol{\Omega}(\boldsymbol{\Omega}+\boldsymbol{I}_K)^{-1}\right]^{\frac{1}{2}} + \widehat{\boldsymbol{G}}_1 \left[(\boldsymbol{\Omega}+\boldsymbol{I}_K)^{-1}\right]^{\frac{1}{2}} \right\} \boldsymbol{\Phi}^{\mathrm{T}} + \sqrt{p_{\mathrm{P}}} \sum_{l=2}^{L} \widehat{\boldsymbol{G}}_l \boldsymbol{\Phi}^{\mathrm{T}} + \boldsymbol{W}_{\mathrm{P}},$$

where $\boldsymbol{W}_{\mathrm{P}}$ is an $N \times K$ noise matrix that satisfies standard complex Gaussian distribution. Removing the LOS part, we get

$$\boldsymbol{Y}_{\mathrm{P}}^{*} = \sqrt{p_{\mathrm{P}}} \widehat{\boldsymbol{G}}_1 \left[(\boldsymbol{\Omega}+\boldsymbol{I}_K)^{-1}\right]^{\frac{1}{2}} \boldsymbol{\Phi}^{\mathrm{T}} + \sqrt{p_{\mathrm{P}}} \sum_{l=2}^{L} \widehat{\boldsymbol{G}}_l \boldsymbol{\Phi}^{\mathrm{T}} + \boldsymbol{W}_{\mathrm{P}}.$$

After correlating the received training signal $\boldsymbol{Y}_{\mathrm{P}}^{*}$ with the pilot sequence of user k, we get

$$\boldsymbol{y}_{\mathrm{P},k}^{*} = \frac{\sqrt{p_{\mathrm{P}}}}{\sqrt{\vartheta_k+1}} \widehat{\boldsymbol{g}}_{1,k} + \sqrt{p_{\mathrm{P}}} \sum_{l=2}^{L} \widehat{\boldsymbol{g}}_{l,k} + \boldsymbol{w}_{\mathrm{P},k},$$

where $\boldsymbol{w}_{\mathrm{P},k} \sim \mathcal{CN}(\boldsymbol{0}, \boldsymbol{I}_N)$. Therefore, according to the LMMSE theory, we get

$$\hat{\widehat{\boldsymbol{g}}}_{l,k} = \begin{cases} \frac{\lambda_{1,k}\boldsymbol{R}}{\sqrt{\vartheta_k+1}} \frac{\boldsymbol{Q}_k}{\sqrt{p_{\mathrm{P}}}} \boldsymbol{y}_{\mathrm{P},k}^{*}, & l=1, \\ \lambda_{l,k}\boldsymbol{R} \frac{\boldsymbol{Q}_k}{\sqrt{p_{\mathrm{P}}}} \boldsymbol{y}_{\mathrm{P},k}^{*}, & l \neq 1, \end{cases}$$

where $\boldsymbol{Q}_k = (\frac{\lambda_{1,k}\boldsymbol{R}}{\vartheta_k+1} + \sum_{l=2}^{L} \lambda_{l,k}\boldsymbol{R} + \frac{\boldsymbol{I}_N}{p_{\mathrm{P}}})^{-1}$. We define $\hat{\boldsymbol{h}}_k \triangleq (\frac{\boldsymbol{Q}_k}{p_{\mathrm{P}}})^{\frac{1}{2}} \boldsymbol{y}_{\mathrm{P},k}^{*} \sim \mathcal{CN}(\boldsymbol{0}, \boldsymbol{I}_N)$ as the Rayleigh fading part of the estimated channel. Thus, $\hat{\widehat{\boldsymbol{g}}}_{l,k}$ can be modeled as

$$\hat{\widehat{\boldsymbol{g}}}_{l,k} = \begin{cases} \frac{\lambda_{1,k}\boldsymbol{R}}{\sqrt{\vartheta_k+1}} \boldsymbol{Q}_k{}^{\frac{1}{2}} \hat{\boldsymbol{h}}_k, & l=1, \\ \lambda_{l,k}\boldsymbol{R}\boldsymbol{Q}_k{}^{\frac{1}{2}} \hat{\boldsymbol{h}}_k, & l \neq 1. \end{cases}$$

Based on the orthogonality property of the LMMSE estimate, $\widehat{\boldsymbol{g}}_{l,k}$ can be decomposed as $\widehat{\boldsymbol{g}}_{l,k} = \hat{\widehat{\boldsymbol{g}}}_{l,k} + \tilde{\widehat{\boldsymbol{g}}}_{l,k}$, where $\tilde{\widehat{\boldsymbol{g}}}_{l,k}$ is the uncorrelated estimation error. Because $\hat{\boldsymbol{g}}_{1,k} = \frac{\hat{\widehat{\boldsymbol{g}}}_{1,k}}{\sqrt{\vartheta_k+1}} + \frac{\sqrt{\vartheta_k}}{\sqrt{\vartheta_k+1}} \bar{\boldsymbol{g}}_{1,k}$, $\tilde{\boldsymbol{g}}_{1,k} = \frac{\tilde{\widehat{\boldsymbol{g}}}_{1,k}}{\sqrt{\vartheta_k+1}}$, and $\hat{\boldsymbol{g}}_{l,k} = \hat{\widehat{\boldsymbol{g}}}_{l,k}$, $\tilde{\boldsymbol{g}}_{l,k} = \tilde{\widehat{\boldsymbol{g}}}_{l,k}$ when $l \neq 1$, the overall estimated channel can be expressed as

$$\hat{\boldsymbol{g}}_{l,k} = \begin{cases} \frac{\lambda_{1,k}\boldsymbol{R}}{\vartheta_k+1} \boldsymbol{Q}_k{}^{\frac{1}{2}} \hat{\boldsymbol{h}}_k + \frac{\sqrt{\vartheta_k}}{\sqrt{\vartheta_k+1}} \bar{\boldsymbol{g}}_{1,k}, & l=1, \\ \lambda_{l,k}\boldsymbol{R}\boldsymbol{Q}_k{}^{\frac{1}{2}} \hat{\boldsymbol{h}}_k, & l \neq 1, \end{cases} \tag{5}$$

and the covariance matrix of the overall estimation error is then expressed as

$$\mathrm{cov}(\tilde{\boldsymbol{g}}_{l,k}, \tilde{\boldsymbol{g}}_{l,k}) = \begin{cases} \frac{\lambda_{1,k}\boldsymbol{R}}{\vartheta_k+1} - \left(\frac{\lambda_{1,k}}{\vartheta_k+1}\right)^2 \boldsymbol{R}\boldsymbol{Q}_k\boldsymbol{R}, & l=1, \\ \lambda_{l,k}\boldsymbol{R} - \lambda_{l,k}^2 \boldsymbol{R}\boldsymbol{Q}_k\boldsymbol{R}, & l \neq 1. \end{cases} \tag{6}$$

3.2 Achievable uplink rate

Considering the uplink transmission represented by (1), the overall uplink received signal at the reference BS can be written as

$$\boldsymbol{y}=\sqrt{p_{\mathrm{u}}}\sum_{i=1}^{K}\hat{\boldsymbol{g}}_{1,i}x_{1,i}+\sqrt{p_{\mathrm{u}}}\sum_{i=1}^{K}\tilde{\boldsymbol{g}}_{1,i}x_{1,i}+\sqrt{p_{\mathrm{u}}}\sum_{l=2}^{L}\sum_{i=1}^{K}\hat{\boldsymbol{g}}_{l,i}x_{l,i}+\sqrt{p_{\mathrm{u}}}\sum_{l=2}^{L}\sum_{i=1}^{K}\tilde{\boldsymbol{g}}_{l,i}x_{l,i}+\boldsymbol{w}.$$

We use an MRC receiver for data detection:

$$\boldsymbol{c}_k=\hat{\boldsymbol{g}}_{1,k}^{\mathrm{H}}=\left(\frac{\hat{\bar{\boldsymbol{g}}}_{1,k}}{\sqrt{\vartheta_k+1}}+\frac{\sqrt{\vartheta_k}}{\sqrt{\vartheta_k+1}}\bar{\boldsymbol{g}}_{1,k}\right)^{\mathrm{H}}.$$

Thus, we get

$$\begin{aligned}r_k=&\sqrt{p_{\mathrm{u}}}\hat{\boldsymbol{g}}_{1,k}^{\mathrm{H}}\hat{\boldsymbol{g}}_{1,k}x_{1,k}+\sqrt{p_{\mathrm{u}}}\hat{\boldsymbol{g}}_{1,k}^{\mathrm{H}}\sum_{i\neq k}^{K}\hat{\boldsymbol{g}}_{1,i}x_{1,i}+\sqrt{p_{\mathrm{u}}}\hat{\boldsymbol{g}}_{1,k}^{\mathrm{H}}\sum_{i=1}^{K}\tilde{\boldsymbol{g}}_{1,i}x_{1,i}\\&+\sqrt{p_{\mathrm{u}}}\sum_{l=2}^{L}\sum_{i=1}^{K}\hat{\boldsymbol{g}}_{1,k}^{\mathrm{H}}\hat{\boldsymbol{g}}_{l,i}x_{l,i}+\sqrt{p_{\mathrm{u}}}\sum_{l=2}^{L}\sum_{i=1}^{K}\hat{\boldsymbol{g}}_{1,k}^{\mathrm{H}}\tilde{\boldsymbol{g}}_{l,i}x_{l,i}+\hat{\boldsymbol{g}}_{1,k}^{\mathrm{H}}\boldsymbol{w}.\end{aligned}$$

Then, the achievable rate of user k is

$$R_k=\mathrm{E}\left[\log_2\left(1+\frac{\left|\hat{\boldsymbol{g}}_{1,k}^{\mathrm{H}}\hat{\boldsymbol{g}}_{1,k}\right|^2}{\hat{\boldsymbol{g}}_{1,k}^{\mathrm{H}}\left(\sum_{l=1}^{L}\sum_{i\neq k}^{K}\hat{\boldsymbol{g}}_{l,i}\hat{\boldsymbol{g}}_{l,i}^{\mathrm{H}}+\sum_{l=1}^{L}\sum_{i=1}^{K}\tilde{\boldsymbol{g}}_{l,i}\tilde{\boldsymbol{g}}_{l,i}^{\mathrm{H}}+\frac{\boldsymbol{I}_N}{p_{\mathrm{u}}}+\sum_{l=2}^{L}\hat{\boldsymbol{g}}_{l,k}\hat{\boldsymbol{g}}_{l,k}^{\mathrm{H}}\right)\hat{\boldsymbol{g}}_{1,k}}\right)\right].$$

Lemma 1. If $X_i, i=1,\ldots,t_1$ and $Y_i, i=1,\ldots,t_2$ are both nonnegative random variables, and $X=\sum_{i=1}^{t_1}X_i$, $Y=\sum_{i=1}^{t_2}Y_i$, then we obtain an approximation as follows [24]:

$$\mathrm{E}\left[\log_2\left(1+\frac{X}{Y}\right)\right]\approx\log_2\left(1+\frac{E[X]}{E[Y]}\right).$$

According to Lemma 1, the achievable rate of user k can be approximated simply as follows.

Theorem 1. For the system model being considered, when BS uses the MRC receiver based on pilot-assisted LMMSE channel estimation, the achievable rate of user k can be approximated simply by

$$R_k\approx\frac{T-K}{T}\log_2\left(1+\widehat{\mathrm{SINR}}_k\right). \tag{7}$$

In order to see the individual effect of the LOS and Rayleigh components on $\widehat{\mathrm{SINR}}_k$, we divide the signal and interfering power into two parts respectively as follows:

$$\widehat{\mathrm{SINR}}_k=\frac{S_{\mathrm{LOS},k}+S_{\mathrm{Ray},k}}{I_{\mathrm{LOS},k}+I_{\mathrm{Ray},k}}, \tag{8}$$

$$\begin{aligned}S_{\mathrm{LOS},k}&=\frac{\lambda_{1,k}^2}{(\vartheta_k+1)^2}\left[2\frac{\vartheta_k}{\vartheta_k+1}\left(N\lambda_{1,k}\sum_{n=1}^{N}\delta_{k,n}^2+\bar{\boldsymbol{g}}_{1,k}^{\mathrm{H}}\boldsymbol{U}\boldsymbol{\Delta}_k^2\boldsymbol{U}^{\mathrm{H}}\bar{\boldsymbol{g}}_{1,k}\right)+\vartheta_k^2N^2\right],\\S_{\mathrm{Ray},k}&=\frac{\lambda_{1,k}^2}{(\vartheta_k+1)^2}\left\{\left(\frac{\lambda_{1,k}}{\vartheta_k+1}\right)^2\left[\sum_{n=1}^{N}\delta_{k,n}^4+\left(\sum_{n=1}^{N}\delta_{k,n}^2\right)^2\right]\right\},\\I_{\mathrm{LOS},k}&=\frac{\vartheta_k}{\vartheta_k+1}\bar{\boldsymbol{g}}_{1,k}^{\mathrm{H}}\left[\boldsymbol{U}\boldsymbol{B}\boldsymbol{U}^{\mathrm{H}}+\sum_{i\neq k}^{K}\left(\frac{\vartheta_i}{\vartheta_i+1}\bar{\boldsymbol{g}}_{1,i}\bar{\boldsymbol{g}}_{1,i}^{\mathrm{H}}\right)\right]\bar{\boldsymbol{g}}_{1,k}\\&\quad+\frac{1}{(\vartheta_k+1)^2}\left[\lambda_{1,k}^2\sum_{i\neq k}^{K}\left(\frac{\vartheta_i}{\vartheta_i+1}\bar{\boldsymbol{g}}_{1,i}^{\mathrm{H}}\boldsymbol{U}\boldsymbol{\Delta}_k^2\boldsymbol{U}^{\mathrm{H}}\bar{\boldsymbol{g}}_{1,i}\right)+\frac{1}{p_{\mathrm{u}}}\vartheta_k(\vartheta_k+1)N\lambda_{1,k}\right],\end{aligned}$$

$$I_{\mathrm{Ray},k}=\frac{\lambda_{1,k}^2}{(\vartheta_k+1)^2}\left\{\sum_{n=1}^{N}a_n\delta_{k,n}^2+\sum_{l=2}^{L}\lambda_{l,k}^2\left[\sum_{n=1}^{N}\delta_{k,n}^4+\left(\sum_{n=1}^{N}\delta_{k,n}^2\right)^2\right]+\frac{\sum_{n=1}^{N}\delta_{k,n}^2}{p_{\mathrm{u}}}\right\},$$

where $\boldsymbol{B}\triangleq\mathbf{A}+\boldsymbol{\Delta}_k^2\sum_{l=2}^{L}\lambda_{l,k}^2$, $\boldsymbol{\Delta}_k=\mathrm{diag}\left(\delta_{k,1},\ldots,\delta_{k,N}\right)$ is a diagonal matrix with element

$$\delta_{k,n}=\frac{d_n}{\sqrt{\frac{\lambda_{1,k}d_n}{\vartheta_k+1}+\sum_{l=2}^{L}\lambda_{l,k}d_n+\frac{1}{p_{\mathrm{P}}}}},\tag{9}$$

$$\begin{aligned}\boldsymbol{A}=&\mathrm{diag}\left(a_1,a_2,\ldots,a_N\right)\\=&\sum_{i=1}^{K}\left(\frac{\lambda_{1,i}\boldsymbol{D}}{\vartheta_i+1}\right)+\sum_{l=2}^{L}\sum_{i=1}^{K}\lambda_{l,i}\boldsymbol{D}-\left(\frac{\lambda_{1,k}}{\vartheta_k+1}\right)^2\boldsymbol{\Delta}_k^2-\sum_{l=2}^{L}\lambda_{l,k}^2\boldsymbol{\Delta}_k^2,\end{aligned}\tag{10}$$

where $\boldsymbol{R}=\boldsymbol{U}\boldsymbol{D}\boldsymbol{U}^{\mathrm{H}}$, with $\boldsymbol{D}=\mathrm{diag}\left(d_1,d_2,\ldots,d_N\right)$.

Proof. See [26].

Theorem 2. When the number of BS antennas is very high, the achievable rate of user k in the reference cell based on pilot-assisted LMMSE channel estimation can be approximated by

$$R_k\to\frac{T-K}{T}\log_2\left(1+\widehat{\mathrm{SINR}}_k^{\infty}\right),\tag{11}$$

where

$$\widehat{\mathrm{SINR}}_k^{\infty}=\frac{\left(\frac{\lambda_{1,k}}{\vartheta_k+1}+\frac{\vartheta_k}{\left(\sum_{n=1}^{N}\delta_{k,n}^2\right)/N}\right)^2}{\sum_{l=2}^{L}\lambda_{l,k}^2}.\tag{12}$$

Proof. See [26].

Reviewing the proof of Theorem 2, we can make the following conclusion.

(1) As the number of BS antennas is very high, the effects of uncorrelated receiver noise and intracell interferences are eliminated completely, leaving the users using the same pilot as the only interferences. This is the same conclusion as for the Rayleigh fading channel. The signal power of the reference user includes both the LOS and Rayleigh components. In addition, when $\vartheta_k=0$,

$$\widehat{\mathrm{SINR}}_k^{\infty}=\frac{\lambda_{1,k}^2}{\sum_{l=2}^{L}\lambda_{l,k}^2},$$

which coincides with the results from the Rayleigh channel.

(2) We further analyze the effect of the LOS component on $\widehat{\mathrm{SINR}}_k^{\infty}$. First, we make the following definitions:

$$\frac{\lambda_{1,k}}{\vartheta_k+1}+\frac{\vartheta_k}{\left(\sum_{n=1}^{N}\frac{d_n^2}{\left(\frac{\lambda_{1,k}}{\vartheta_k+1}+\sum_{l=2}^{L}\lambda_{l,k}\right)d_n+\frac{1}{p_{\mathrm{P}}}}\right)\Big/N}\triangleq x,$$

$$\frac{\vartheta_k}{\left(\sum_{n=1}^{N}\frac{d_n^2}{\left(\frac{\lambda_{1,k}}{\vartheta_k+1}+\sum_{l=2}^{L}\lambda_{l,k}\right)d_n+\frac{1}{p_{\mathrm{P}}}}\right)\Big/N}\triangleq y.$$

After performing some algebraic operation to y, we get

$$y=\frac{1}{\sum_{n=1}^{N}\frac{d_n^2/N}{\frac{\vartheta_k\lambda_{1,k}d_n}{\vartheta_k+1}+\vartheta_k\left(\sum_{l=2}^{L}\lambda_{l,k}d_n+\frac{1}{p_{\mathrm{P}}}\right)}},$$

which shows that with the increase in ϑ_k, $\frac{\vartheta_k}{\vartheta_k+1}$ increases, which in turn causes y to increase. In addition, the increase in y consists of the increase in $\frac{\vartheta_k\lambda_{1,k}d_n}{\vartheta_k+1}$ and $\vartheta_k(\sum_{l=2}^{L}\lambda_{l,k}d_n+\frac{1}{p_{\mathrm{P}}})$. Because

$$\frac{1}{\sum_{n=1}^{N}\frac{d_n^2/N}{\frac{\vartheta_k\lambda_{1,k}d_n}{\vartheta_k+1}+\vartheta_k\left(\sum_{l=2}^{L}\lambda_{l,k}d_n+\frac{1}{p_{\mathrm{P}}}\right)}}\geqslant\frac{1}{\sum_{n=1}^{N}\frac{d_n^2/N}{\frac{\vartheta_k\lambda_{1,k}d_n}{\vartheta_k+1}}}=\frac{\vartheta_k\lambda_{1,k}}{\vartheta_k+1},$$

and $\frac{\lambda_{1,k}}{\vartheta_k+1}+\frac{\vartheta_k\lambda_{1,k}}{\vartheta_k+1}=\lambda_{1,k}$ is independent of ϑ_k, then we can conclude that x increases with the increase in ϑ_k, which means the LOS component raises the user's SINR.

(3) If $\sum_{m=1}^{M} x_m = M$, for any $a>0,\ b>0,\ x_m>0$, we have

$$\frac{M^2}{aM+b} > \sum_{m=1}^{M} \frac{x_m^2}{ax_m+b} \geqslant \frac{M}{a+b}, \tag{13}$$

and the upper limit of the this inequality is achieved when $x_i = M$ and $x_m = 0, m \neq i$, whereas the lower limit is achieved when $x_i = 1, \forall i$. According to (12), the LOS component of the signal power is related to the correlation of the BS antennas, whereas the Rayleigh component is independent of the correlation. In addition, according to (13), we get

$$\frac{1}{\frac{\lambda_{1,k}}{\vartheta_k+1}+\sum_{l=2}^{L}\lambda_{l,k}} > \frac{\sum_{n=1}^{N}\delta_{k,n}^2}{N} \geqslant \frac{1}{\frac{\lambda_{1,k}}{\vartheta_k+1}+\sum_{l=2}^{L}\lambda_{l,k}+\frac{1}{p_{\mathrm{P}}}},$$

Thus, in the case of a large p_{P}, we can conclude that the correlation of BS antennas has little influence on the asymptotic rate. In addition, the asymptotic rate is nearly independent of the value of p_{P}.

When $\boldsymbol{R}=\boldsymbol{I}$, after some algebraic manipulations, $\widehat{\mathrm{SINR}}_k^{\infty}$ can be expressed as

$$\widehat{\mathrm{SINR}}_k^{\infty} = \frac{\left[\lambda_{1,k}+\vartheta_k\left(\sum_{l=2}^{L}\lambda_{l,k}+\frac{1}{p_{\mathrm{P}}}\right)\right]^2}{\sum_{l=2}^{L}\lambda_{l,k}^2}, \tag{14}$$

which coincides with [24]. In addition, the expression confirms our conclusion that the LOS componet raises the user's SINR.

Theorem 3. If the transmit power of each user is scaled down to $p_{\mathrm{u}} = E_{\mathrm{u}}N^{-\varepsilon}$ for a fixed E_{u} and $\varepsilon>0$, when the number of antennas increases, the user's uplink rate of the MRC receiver based on pilot-assisted LMMSE channel estimate approaches the following:

$$R_k \to \frac{T-K}{T}\log_2\left(1+\widehat{\mathrm{SINR}}_k^{\mathrm{ps}}\right), \tag{15}$$

where

$$\widehat{\mathrm{SINR}}_k^{\mathrm{ps}} = \frac{N^{1-\varepsilon}E_{\mathrm{u}}\lambda_{1,k}\vartheta_k}{(\vartheta_k+1)}, \tag{16}$$

and for $\vartheta_k = 0$,

$$\mathrm{SINR}_k^{\mathrm{ps}} = \frac{\lambda_{1,k}^2}{\sum_{l=2}^{L}\lambda_{l,k}^2+\frac{1}{KE_{\mathrm{u}}^2N^{-2\varepsilon}\sum_{n=1}^{N}d_n^2}}. \tag{17}$$

Proof. See [26].

We can make several observations from Theorem 3. For Rayleigh fading, the SINR is dependent on the BS-sided correlation when the power scaling is considered (although the effect is limited). In addition, ε should be no more than 1/2 to obtain a non-zero constant value with increasing N. For Ricean fading, the SINR is independent of the BS-sided correlation when the power scaling is considered. Furthermore, ε should be no more than 1 in order to obtain a non-zero constant value with increasing N. Comparing (16) and (17), we find that for Ricean fading, the uplink rate depends only on the LOS related power, whereas the Rayleigh related power and the interference from users in other cells disappear.

4 Uplink rate analysis using LOS component as channel estimate

The received signal $\boldsymbol{y}$ can be expressed in the following form:

$$\boldsymbol{y} = \sqrt{p_{\mathrm{u}}}\sum_{i=1}^{K}\frac{\sqrt{\vartheta_i}}{\sqrt{\vartheta_i+1}}\bar{\boldsymbol{g}}_{1,i}x_{1,i} + \sqrt{p_{\mathrm{u}}}\sum_{i=1}^{K}\frac{\widehat{\boldsymbol{g}}_{1,i}x_{1,i}}{\sqrt{\vartheta_i+1}} + \sqrt{p_{\mathrm{u}}}\sum_{l=2}^{L}\sum_{i=1}^{K}\boldsymbol{g}_{l,i}x_{l,i} + \boldsymbol{w}.$$

As previously mentioned, both the deterministic LOS component and Ricean factor matrix $\boldsymbol{\Omega}$ are perfectly known. In this section we use the LOS component as the channel estimate while using the scattered part as interference. Let $\boldsymbol{z} = \sqrt{p_{\mathrm{u}}}\sum_{i=1}^{K}\frac{\widehat{\boldsymbol{g}}_{1,i}x_{1,i}}{\sqrt{\vartheta_i+1}} + \sqrt{p_{\mathrm{u}}}\sum_{l=2}^{L}\sum_{i=1}^{K}\boldsymbol{g}_{l,i}x_{l,i} + \boldsymbol{w}$ identified as the effective noise with covariance

$$\boldsymbol{\Omega} = E\left(\boldsymbol{z}\boldsymbol{z}^{\mathrm{H}}\right) = p_{\mathrm{u}}\sum_{i=1}^{K}\frac{\lambda_{1,i}}{\vartheta_i+1} + p_{\mathrm{u}}\sum_{l=2}^{L}\sum_{i=1}^{K}\lambda_{l,k}\boldsymbol{R} + \boldsymbol{I}_N.$$

Based on the assumptions, the MRC filter $\bar{\boldsymbol{c}}_k = \bar{\boldsymbol{g}}_{1,k}^{\mathrm{H}}$. Thus, after MRC filtering, the signal of the kth user is

$$r_k = \sqrt{p_{\mathrm{u}}}\frac{\sqrt{\vartheta_k}\bar{\boldsymbol{g}}_{1,k}^{\mathrm{H}}\bar{\boldsymbol{g}}_{1,k}x_{1,k}}{\sqrt{\vartheta_k+1}} + \frac{\bar{\boldsymbol{g}}_{1,k}^{\mathrm{H}}\widehat{\boldsymbol{g}}_{1,k}x_{1,k}}{\sqrt{\vartheta_k+1}} + \sqrt{p_{\mathrm{u}}}\sum_{i\neq k}^{K}\bar{\boldsymbol{g}}_{1,k}^{\mathrm{H}}\boldsymbol{g}_{1,i}x_{1,i} + \sqrt{p_{\mathrm{u}}}\sum_{l=2}^{L}\sum_{i=1}^{K}\bar{\boldsymbol{g}}_{1,k}^{\mathrm{H}}\boldsymbol{g}_{l,i}x_{l,i} + \bar{\boldsymbol{g}}_{1,k}^{\mathrm{H}}\boldsymbol{w}.$$

Based on the Worst Case Uncorrelated Additive Noise Theorem, the lower bound of the kth user's achievable rate is

$$R_k = \log_2\left(1 + \frac{\frac{\vartheta_k}{\vartheta_k+1}\left|\bar{\boldsymbol{g}}_{1,k}^{\mathrm{H}}\bar{\boldsymbol{g}}_{1,k}\right|^2}{E\left[\bar{\boldsymbol{g}}_{1,k}^{\mathrm{H}}\left(\frac{\widehat{\boldsymbol{g}}_{1,k}\widehat{\boldsymbol{g}}_{1,k}^{\mathrm{H}}}{\vartheta_k+1} + \sum_{i\neq k}^{K}\boldsymbol{g}_{1,i}\boldsymbol{g}_{1,i}^{\mathrm{H}} + \sum_{l=2}^{L}\sum_{i=1}^{K}\boldsymbol{g}_{l,i}\boldsymbol{g}_{l,i}^{\mathrm{H}} + \frac{\boldsymbol{I}_N}{p_{\mathrm{u}}}\right)\bar{\boldsymbol{g}}_{1,k}\right]}\right).$$

Theorem 4. For the system model considered, when the BS uses the MRC receiver based on the LOS component, the lower bound of the achievable rate of user k is

$$R_k = \log_2\left(1 + \overline{\mathrm{SINR}}_k\right), \tag{18}$$

where

$$\overline{\mathrm{SINR}}_k = \frac{\frac{\vartheta_k}{\vartheta_k+1}(\lambda_{1,k}N)^2}{\lambda_{1,k}\sum_{i\neq k}^{K}\frac{\vartheta_i\lambda_{1,i}}{\vartheta_i+1}|\rho_{k,i}|^2 + \sum_{i=1}^{K}\frac{\lambda_{1,i}\bar{\boldsymbol{g}}_{1,k}^{\mathrm{H}}\boldsymbol{R}\bar{\boldsymbol{g}}_{1,k}}{\vartheta_i+1} + \sum_{l=2}^{L}\sum_{i=1}^{K}\lambda_{l,i}\bar{\boldsymbol{g}}_{1,k}^{\mathrm{H}}\boldsymbol{R}\bar{\boldsymbol{g}}_{1,k} + \frac{\lambda_{1,k}N}{p_{\mathrm{u}}}}, \tag{19}$$

$$\rho_{k,i} = \frac{1-\mathrm{e}^{\mathrm{j}N\varphi_{ki}}}{1-\mathrm{e}^{\mathrm{j}\varphi_{ki}}}, \tag{20}$$

$$\varphi_{ki} = \frac{2\pi d}{\lambda}\left(\sin\theta_k - \sin\theta_i\right). \tag{21}$$

Proof. Define

$$\overline{\mathrm{SINR}}_k \triangleq \frac{\frac{\vartheta_k}{\vartheta_k+1}\left|\bar{\boldsymbol{g}}_{1,k}^{\mathrm{H}}\bar{\boldsymbol{g}}_{1,k}\right|^2}{E\left[\bar{\boldsymbol{g}}_{1,k}^{\mathrm{H}}\left(\frac{\widehat{\boldsymbol{g}}_{1,k}\widehat{\boldsymbol{g}}_{1,k}^{\mathrm{H}}}{\vartheta_k+1} + \sum_{i\neq k}^{K}\boldsymbol{g}_{1,i}\boldsymbol{g}_{1,i}^{\mathrm{H}} + \sum_{l=2}^{L}\sum_{i=1}^{K}\boldsymbol{g}_{l,i}\boldsymbol{g}_{l,i}^{\mathrm{H}} + \frac{\boldsymbol{I}_N}{p_{\mathrm{u}}}\right)\bar{\boldsymbol{g}}_{1,k}\right]}, \tag{22}$$

and then each element of the numerator and denominator can be simplified as follows:

$$\left|\bar{\boldsymbol{g}}_{1,k}^{\mathrm{H}}\bar{\boldsymbol{g}}_{1,k}\right|^2 = (\lambda_{1,k}N)^2,$$

$$E\left[\bar{\boldsymbol{g}}_{1,k}^{\mathrm{H}}\left(\frac{\boldsymbol{I}_N}{p_{\mathrm{u}}}\right)\bar{\boldsymbol{g}}_{1,k}\right] = \frac{\lambda_{1,k}N}{p_{\mathrm{u}}},$$

$$\mathrm{E}\left[\bar{\boldsymbol{g}}_{1,k}^{\mathrm{H}}\frac{\widehat{\boldsymbol{g}}_{1,k}\widehat{\boldsymbol{g}}_{1,k}^{\mathrm{H}}}{\vartheta_k+1}\bar{\boldsymbol{g}}_{1,k}\right] = \frac{\lambda_{1,k}\bar{\boldsymbol{g}}_{1,k}^{\mathrm{H}}\boldsymbol{R}\bar{\boldsymbol{g}}_{1,k}}{\vartheta_k+1},$$

$$\mathrm{E}\left[\bar{\boldsymbol{g}}_{1,k}^{\mathrm{H}}\left(\sum_{l=2}^{L}\sum_{i=1}^{K}\boldsymbol{g}_{l,i}\boldsymbol{g}_{l,i}^{\mathrm{H}}\right)\bar{\boldsymbol{g}}_{1,k}\right] = \sum_{l=2}^{L}\sum_{i=1}^{K}\lambda_{l,i}\bar{\boldsymbol{g}}_{1,k}^{\mathrm{H}}\boldsymbol{R}\bar{\boldsymbol{g}}_{1,k},$$

$$\mathrm{E}\left[\bar{\boldsymbol{g}}_{1,k}^{\mathrm{H}}\left(\sum_{i\neq k}^{K}\boldsymbol{g}_{1,i}\boldsymbol{g}_{1,i}^{\mathrm{H}}\right)\bar{\boldsymbol{g}}_{1,k}\right]=\lambda_{1,k}\sum_{i\neq k}^{K}\frac{\vartheta_i\lambda_{1,i}}{\vartheta_i+1}|\rho_{k,i}|^2+\sum_{i\neq k}^{K}\frac{\lambda_{1,i}\bar{\boldsymbol{g}}_{1,k}^{\mathrm{H}}\boldsymbol{R}\bar{\boldsymbol{g}}_{1,k}}{\vartheta_i+1}.$$

Then, substituting all the expressions into (22), Theorem 4 is proved.

Similarly, we give the expression of $\mathrm{SINR}_k^{\mathrm{LOS}}$ when the number of BS antennas N is high.

Theorem 5. Using the LOS component as the channel estimate, as the number of BS antennas N is very high, the achievable rate of user k can be approximated as follows:

$$R_k\to\log_2\left(1+\overline{\mathrm{SINR}}_k^{\infty}\right),\tag{23}$$

where

$$\overline{\mathrm{SINR}}_k^{\infty}=\frac{\frac{\vartheta_k}{\vartheta_k+1}\left(\lambda_{1,k}N\right)}{\sum_{i=1}^{K}\frac{\lambda_{1,i}\bar{\boldsymbol{g}}_{1,k}^{\mathrm{H}}\boldsymbol{R}\bar{\boldsymbol{g}}_{1,k}}{N\lambda_{1,k}(\vartheta_i+1)}+\sum_{l=2}^{L}\sum_{i=1}^{K}\frac{\lambda_{l,i}\bar{\boldsymbol{g}}_{1,k}^{\mathrm{H}}\boldsymbol{R}\bar{\boldsymbol{g}}_{1,k}}{N\lambda_{1,k}}+\frac{1}{p_{\mathrm{u}}}}.\tag{24}$$

Proof. Since $d_{\min}N\lambda_{1,k}\leqslant\bar{\boldsymbol{g}}_{1,k}^{\mathrm{H}}\boldsymbol{R}\bar{\boldsymbol{g}}_{1,k}\leqslant d_{\max}N\lambda_{1,k}$, we define $\bar{\boldsymbol{g}}_{1,k}^{\mathrm{H}}\boldsymbol{R}\bar{\boldsymbol{g}}_{1,k}=\alpha\lambda_{l,k}N$, $\alpha>0$ and limited, which depends on the BS-sided correlation. Therefore, $\frac{\bar{\boldsymbol{g}}_{1,k}^{\mathrm{H}}\boldsymbol{R}\bar{\boldsymbol{g}}_{1,k}}{N}$ is a constant depending on the BS-sided correlation. In addition, $\rho_{k,i}=\frac{1-\mathrm{e}^{\mathrm{j}N\varphi_{ki}}}{1-\mathrm{e}^{\mathrm{j}\varphi_{ki}}}$, $\varphi_{ki}=\frac{2\pi d}{\lambda}\left(\sin\theta_k-\sin\theta_i\right)$ and $\left|1-\mathrm{e}^{\mathrm{j}N\varphi_{ki}}\right|$ are limited. Therefore, when $N\to\infty$, $\frac{|\rho_{k,i}|^2}{N}\to 0$. Finally, Theorem 5 is proved.

Theorem 5 shows that as the number of BS antennas is very high, the power of the reference user increases linearly with the number of BS antennas; the intracell interferences caused by the LOS component are eliminated completely, leaving the power related to the Rayleigh component of all users and the uncorrelated noise as the finite interferences. In addition, compared to the power related to the Rayleigh component, the noise power has little influence on the asymptotic rate in the case of a large p_{u}. Based on these, we can easily speculate that as the number of BS antennas increases considerably, the user's rate when using the LOS component will gradually exceed the rate when using the LMMSE estimate. Moreover, according to (24), the rate increases with the increase in ϑ.

For $\boldsymbol{R}=\boldsymbol{I}$, Eq. (24) becomes

$$\overline{\mathrm{SINR}}_k^{\infty}=\frac{\frac{\vartheta_k}{\vartheta_k+1}\left(\lambda_{1,k}N\right)}{\sum_{i=1}^{K}\frac{\lambda_{1,i}}{(\vartheta_i+1)}+\sum_{l=2}^{L}\sum_{i=1}^{K}\lambda_{l,i}+\frac{1}{p_{\mathrm{u}}}}.\tag{25}$$

Eq. (25) shows clearly that with the increase in the number of BS antennas, the user's SINR of the reference cell increases linearly when using the LOS component as the channel estimate.

Theorem 6. If the transmit power of each user is scaled down to $p_{\mathrm{u}}=E_{\mathrm{u}}N^{-\varepsilon}$ for a fixed E_{u} and $\varepsilon>0$, when the number of antennas increases, the user's uplink rate of the MRC receiver based on the LOS component as the channel estimate approaches the following:

$$R_k\to\log_2\left(1+\overline{\mathrm{SINR}}_k^{\mathrm{ps}}\right),\tag{26}$$

where

$$\overline{\mathrm{SINR}}_k^{\mathrm{ps}}=\frac{\vartheta_k\lambda_{1,k}E_{\mathrm{u}}}{\vartheta_k+1}N^{1-\varepsilon}.\tag{27}$$

Proof. Subsituting $p_{\mathrm{u}}=E_{\mathrm{u}}N^{-\varepsilon}$ into (19),

$$\mathrm{SINR}_k^{\mathrm{LOS}}=\frac{\frac{\vartheta_k}{\vartheta_k+1}(\lambda_{1,k}N)^2}{\frac{\lambda_{1,k}\bar{\boldsymbol{g}}_{1,k}^{\mathrm{H}}\boldsymbol{R}\bar{\boldsymbol{g}}_{1,k}}{\vartheta_k+1}+\lambda_{1,k}\sum_{i\neq k}^{K}\frac{\vartheta_i\lambda_{1,i}}{\vartheta_i+1}|\rho_{k,i}|^2+\sum_{i\neq k}^{K}\frac{\lambda_{1,i}\bar{\boldsymbol{g}}_{1,k}^{\mathrm{H}}\boldsymbol{R}\bar{\boldsymbol{g}}_{1,k}}{\vartheta_i+1}+\sum_{l=2}^{L}\sum_{i=1}^{K}\lambda_{l,i}\bar{\boldsymbol{g}}_{1,k}^{\mathrm{H}}\boldsymbol{R}\bar{\boldsymbol{g}}_{1,k}+\frac{\lambda_{1,k}N^{1+\varepsilon}}{E_{\mathrm{u}}}}$$

similar to the proof of Theorem 5, when $N\to\infty$,

$$\mathrm{SINR}_k^{\mathrm{LOS}}\to\frac{\vartheta_k\lambda_{1,k}E_{\mathrm{u}}}{\vartheta_k+1}N^{1-\varepsilon}\triangleq\overline{\mathrm{SINR}}_k^{\mathrm{ps}}.$$

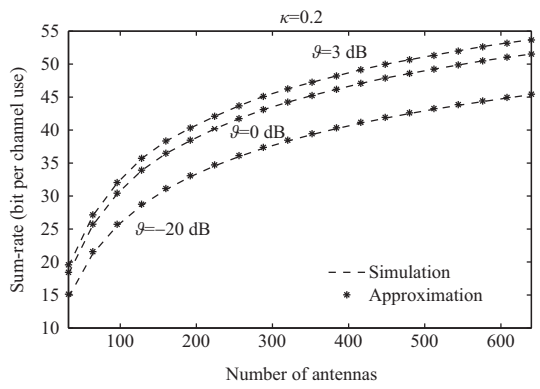

Figure 1 Uplink sum-rate as a function of the number of BS antennas N for various Ricean factors when the pilot-assisted LMMSE estimation is used with $\kappa = 0.2$.

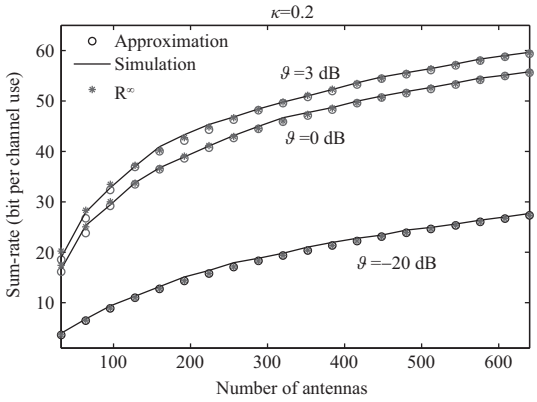

Figure 2 Uplink sum-rate as a function of the number of BS antennas N for various Ricean factors when the LOS component is used for channel estimation with $\kappa = 0.2$.

Thus, Theorem 6 is proved.

We find that Eq. (27) is the same as (16). Therefore, we conclude that for a Ricean channel, when power scaling is considered, pilot contamination will gradually disappear using pilot-assisted LMMSE channel estimation, and the user's SINR will approach to that when using the LOS component as channel estimation. Thus, for massive MIMO, pilot-assisted LMMSE estimation has little meaning.

5 Numerical results

In this section, we validate the aforementioned analyses presented through a set of Monte-Carlo simulations. As in [27], a 7-cell hexagonal system layout is adopted. The inner cell radius is normalized to 1, the distance between two adjacent cells is normalized to 2, and we assume a distance-based path loss model with path loss exponent $\alpha = 3.7$. To enable our results to be reproduced, we distribute $K = 10$ users uniformly on a circle of radius 2/3 around each BS based on the random position distribution model in [27]. The entries of the BS-sided correlation matrix are modeled via the common exponential correlation model $[\boldsymbol{R}_{l,i}]_{m,n} = \kappa^{|m-n|}$ with κ being the correlation coefficient. Assuming all users in the reference cell have the identical Ricean factor, and with the ratio of the antenna spacing to wavelength set to 0.5, unless otherwise stated, the arrival angles are uniformly distributed in the interval $\left[-\frac{\pi}{2}, \frac{\pi}{2}\right)$, which means $\theta_k = \frac{\pi(k-1)}{K} - \frac{\pi}{2}, k = 1, \ldots, K$. In addition, the coherence time of the channel is chosen as $T = 196$ according to the long term evolution (LTE) standard.

We next give a comparison of the two methods of channel estimation. First, we assess the validity of the proposed approximate formulas. Assuming the data power $p_{\mathrm{u}} = 10$ dB, and the pilot power $p_{\mathrm{P}} = 10p_{\mathrm{u}}$, Figure 1 plots the achievable sum-rate against the number of BS antennas N for various Ricean factors when the pilot-assisted LMMSE estimation is used with $\kappa = 0.2$. Obviously, the approximate expression is quite tight, especially at a large N. Figure 1 shows that, as expected, the achievable rate increases with an increase in the Ricean factor ϑ_k, which is consistent with the aforementioned conclusion that the uplink rate with Ricean fading is higher than that with Rayleigh fading. Figure 2 plots the achievable sum-rate against N for various Ricean factors when the LOS component is used for channel estimation with $\kappa = 0.2$. Similarly, the approximate expression is quite tight, especially at a large N. Figure 2 shows that, as expected, the achievable rate increases with an increase in the Ricean factor ϑ_k. Moreover, we find that Eq. (18) approaches the asymptotic rate (23) when the number of antennas is not very high.

Figure 3 plots the achievable sum-rate against SNR for different numbers of antennas N with $\kappa = 0.2$, $\vartheta_k = 3$ dB for pilot-assisted LMMSE estimation and the LOS component channel as channel estimation. Because the power of the noise is normalized, the value of SNR equals p_{u}. Obviously, the approximate expressions are quite tight for different SNR, especially at a large N. Therefore, as explained in the

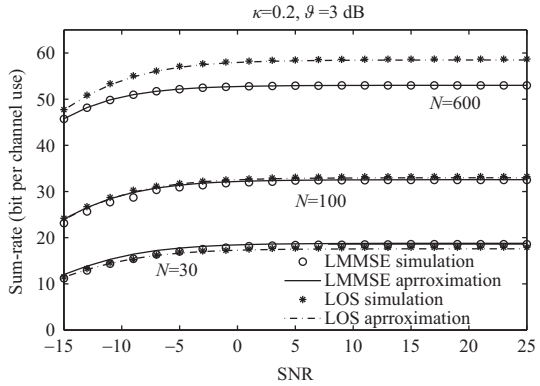

Figure 3 Uplink sum-rate against SNR for different numbers of antennas N with $\kappa = 0.2$, $\vartheta_k = 3$ dB for pilot-assisted LMMSE estimation and the LOS component channel as channel estimation.

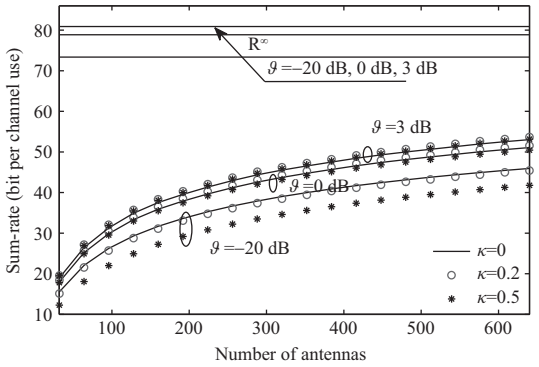

Figure 4 Uplink sum-rate as a function of the number of BS antennas N for various Ricean factors and various correlation coefficients when the pilot assisted LMMSE estimation is used.

following section, we use the approximate expression to replace the exact one for performance analysis. As expected, the increase in SNR raises the achievable sum-rate. However, the effect is gradually weakened as the SNR grows. In addition, in the case of a large SNR, the achievable sum-rate is practically independent of SNR. Figure 3 shows that the achievable sum-rate increases with the increase in N for both channel estimation methods. The influence of N is also greater when LOS is used for channel estimation compared with the pilot-assisted LMMSE channel estimation, which causes the sum-rate of LOS to gradually exceed that of the pilot-assisted LMMSE channel estimation.

For further analysis of the effect of the BS correlation on the uplink sum-rate, Figure 4 plots the achievable sum-rate as a function of the number of BS antennas N for various Ricean factors and correlation coefficients. R^{∞} is the asymptotic sum-rate when N is very high. When N is finite, Figure 4 clearly shows that for small ϑ_k (that is, near Rayleigh fading) the correlation decreases the uplink rate. However, as ϑ_k increases, the effect of correlation on the uplink sum-rate becomes varied; it seems that the correlation causes a light increase. As expected, when N is very high, the infinite rates for different correlations are too similar to be distinguished in the plot, which means that the effect of the BS spatial correlation on the rate can be negligible.

In order to provide an assessment of the influence of spatial correlation on the uplink sum-rate, Figure 5(a) plots the achievable sum-rate as a function of the number of BS antennas N for various Ricean factors and correlation coefficients. Figure 5(a) clearly shows that the correlation increases the uplink sum-rate, and the increased phenomenon is not eliminated with the increase in the number of antennas. Through further analysis, we find that the phenomenon is not inevitable, as it depends on the position distribution of users. For example, if we choose $\theta_k = \frac{2k-1}{2K} - \frac{\pi}{4}, k = 1, \ldots, K$, the correlation decreases the uplink sum-rate, as shown in Figure 5(b).

For further analysis of the effect of spatial correlation and the Ricean factor on the sum-rate, Figure 6 shows the sum-rate against the Ricean factor ϑ_k for different correlation coefficients with $N = 600$ for two channel estimation methods. By fully analyzing the two groups of curves, we can derive the following conclusion. For a Ricean channel, the spatial correlation can either decrease or increase the sum-rate depending on the distribution of the user positions. For the Rayleigh fading channel, the spatial correlation only decreases the sum-rate. If the specific position distribution causes the LOS component related sum-rate to increase, then the effect of the LOS component on the sum-rate grows with the increase in Ricean factor. Finally, the total sum-rate with pilot-assisted LMMSE estimation increases, as shown in Figure 6.

Figure 7 validates the power-scaling law in Theorems 3 and 6 with $\vartheta_k = 6$ dB, $E_{\mathrm{u}} = 20$ dB. When the scaling factor $\varepsilon = 1$, the sum-rate against the number of antennas shows a trend of rising to a level of stability. However, when $\varepsilon = 1.5$, the sum-rate against the number of antennas shows a trend in which it

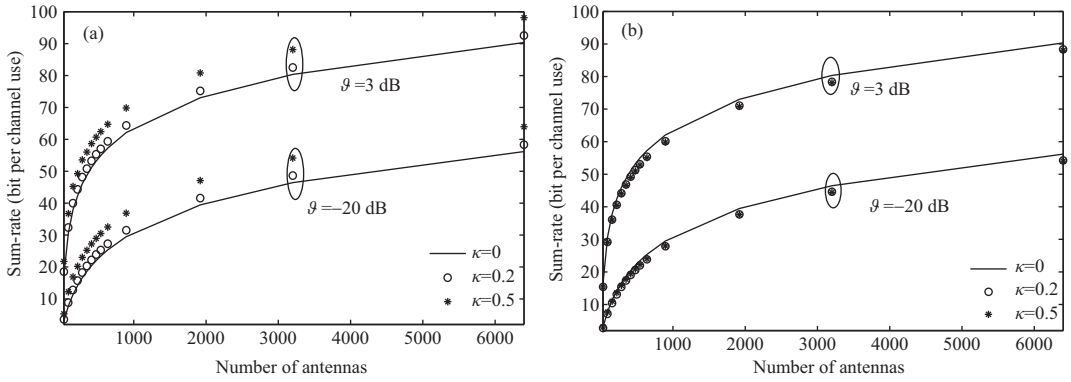

Figure 5 Effect of user position distribution on the sum-rate when the LOS component is used for channel estimation. (a) $\theta_k=\frac{\pi(k-1)}{K}-\frac{\pi}{2}, k=1,\ldots,K$; (b) $\theta_k=\frac{2k-1}{2K}-\frac{\pi}{4}, k=1,\ldots,K$.

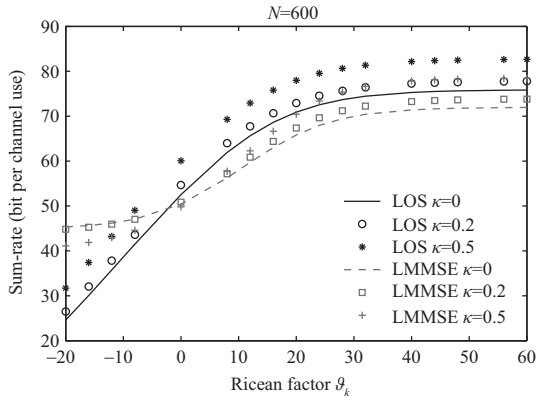

Figure 6 Uplink sum-rate against the Ricean factor ϑ_k for different correlation coefficients with $N = 600$ for two channel estimation methods.

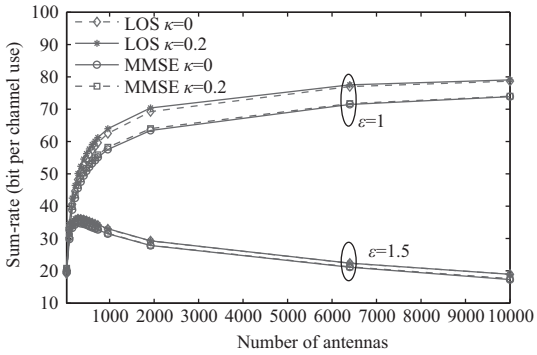

Figure 7 Comparison of uplink sum-rates as a function of the number of BS antennas N between pilot-assisted LMMSE estimation and the LOS component channel for channel estimation when power scaling is taken.

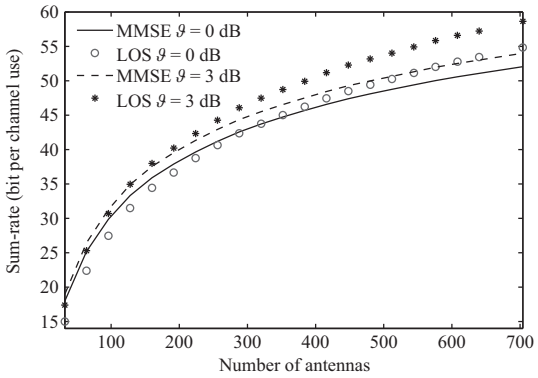

Figure 8 Comparison of uplink sum-rates as a function of the number of BS antennas N between pilot-assisted LMMSE estimation and the LOS component channel for channel estimation.

first rises, then declines, which means the user's power has been reduced too much. In addition, when the transmit power is scaled, the sum-rates of the two methods eventually become identical as N increases (in Figure 7, $N = 1200$). The difference between the two methods is because of the pilot overhead ($\frac{T-K}{T}$). Figure 7 also shows that the spacial correlation has little influence on the power-scaled sum-rate.

Figure 8 compares the sum-rate against the number of antennas for the two methods of channel estimation. Figure 8 clearly shows that with the increase in N, the gap between the two methods is

gradually reduced, and after a specific value (we simply call it the turning point), the sum-rate when LOS is used as channel estimation becomes greater than that of the pilot-assisted LMMSE channel estimation. Moreover, the bigger ϑ_k is, the smaller is the value of the turning point.

6 Conclusion

We studied the performances of spectral efficiency over a correlated Ricean fading channel. We deduced the respective analytical expressions for two methods. The first method was MRC based on pilot-assisted LMMSE estimation. The second method was MRC based on LOS component. The effect of Ricean fading was investigated extensively in the study. The following conclusion was drawn.

(1) When the number of BS antennas is very high, as a result of pilot contamination, the asymptotic uplink data rate of the pilot-assisted LMMSE estimation method approaches a finite value, which increases with an increase in the Ricean factor. However, the asymptotic uplink data rate of the LOS method is linearly with the number of BS antennas. Therefore, the uplink achievable rate of the LOS method will exceed that of the pilot-assisted LMMSE estimation method with the increase in the number of antennas.

(2) The expression of the achievable rate of the LOS method also showed the correlation between the BS antennas may either decrease or increase the rate depending on user location. Therefore, if the locations of the users cause antenna correlation to increase the rate, with an increase in the Ricean factor, the rate of pilot-assisted LMMSE estimation method will increase as a result of antenna correlation, as the effect of LOS component becomes stronger.

(3) When the power is scaled, the asymptotic expressions of the two methods are the same and both are independent of antenna correlation.

(4) In summary, when the power of LOS component is comparable to that of the Rayleigh component in Ricean channel, it has little meaning for pilot-assisted LMMSE estimation for massive MIMO.

Acknowledgements This work was supported in part by Natural Science Foundation of China (Grant Nos. 61501113, 61521061, 61401241, 61501264), Natural Science Foundation of Jiangsu Province (Grant No. BK201506-30), and Open Research Fund of National Mobile Communications Research Laboratory, Southeast University (Grant No. 2015D02).

References

1 Feng W, Wang Y, Ge N, et al. Virtual MIMO in multi-cell distributed antenna systems: coordinated transmissions with large-scale CSIT. IEEE J Sel Areas Commun, 2013, 31: 2067–2081
2 Yang A, Xing C W, Fei Z S, et al. Performance analysis for uplink massive MIMO systems with a large and random number of UEs. Sci China Inf Sci, 2016, 59: 022312
3 Wang D M, Zhang Y, Wei H, et al. An overview of transmission theory and techniques of large-scale antenna systems for 5G wireless communications. Sci China Inf Sci, 2016, 59: 081301
4 Wang X Y, Zhang Z S, Long K P, et al. Joint group power allocation and prebeamforming for joint spatial-division multiplexing in multiuser massive MIMO systems. In: Proceedings of 2015 IEEE International Conference on Acoustics, Speech and Signal Processing (ICASSP), Brisbane, 2015. 2934–2938
5 Boccardi F, Heath R W, Lozano A, et al. Five disruptive technology directions for 5G. IEEE Commun Mag, 2014, 52: 74–80
6 Jose J, Ashikhmin A, Marzetta T L, et al. Pilot contamination and precoding in multi-cell TDD systems. IEEE Trans Wirel Commun, 2011, 10: 2640–2651
7 Appaiah K, Ashikhmin A, Marzetta T L. Pilot contamination reduction in multi-user TDD systems. In: Proceedings of 2010 IEEE International Conference on Communications (ICC), Cape Town, 2010. 1–5
8 Fernandes F, Ashikhmin A, Marzetta T L. Inter-cell interference in noncooperative TDD large scale antenna systems. IEEE J Sel Areas Commun, 2013, 31: 192–201
9 Li M M, Jin S, Gao X Q. Spatial orthogonality-based pilot reuse for multi-cell massive MIMO transmission. In: Proceedings of 2013 International Conference on Wireless Communications Signal Processing (WCSP), Hangzhou, 2013. 1–6
10 Wang H R, Huang Y M, Jin S, et al. Performance analysis on precoding and pilot scheduling in very large MIMO multi-cell systems. In: Proceedings of Wireless Communications and Networking Conference (WCNC), Shanghai, 2013. 2722–2726

11 Yue S S, Liu J, Zhai C, et al. User pilot scheduling in massive MIMO systems. In: Proceedings of 2015 International Conference on Wireless Communications Signal Processing (WCSP), Nanjing, 2015. 1–5
12 Zhu X, Wang Z, Dai L, et al. Smart pilot assignment for massive MIMO. IEEE Commun Lett, 2015, 19: 1644–1647
13 Yin H, Gesbert D, Filippou M, et al. A coordinated approach to channel estimation in large-scale multiple-antenna systems. IEEE J Sel Areas Commun, 2013, 31: 264–273
14 Ngo H Q, Larsson E G. EVD-based channel estimation in multicell multiuser MIMO systems with very large antenna arrays. In: Proceedings of 2012 IEEE International Conference on Acoustics, Speech and Signal Processing (ICASSP), Kyoto, 2012. 3249–3252
15 Muller R R, Vehkapera M, Cottatellucci L. Blind pilot decontamination. In: Proceedings of the 17th International ITG Workshop on Smart Antennas (WSA 2013), Stuttgart, 2013. 1–6
16 Muller R R, Cottatellucci L, Vehkapera M. Blind pilot decontamination. IEEE J Sel Top Signal Process, 2014, 8: 773–786
17 Donoho D L. Compressed sensing. IEEE Trans Inform Theor, 2006, 52: 1289–1306
18 Wu L, Qi C. Uplink channel estimation for massive MIMO systems exploring joint channel sparsity. Electron Lett, 2014, 50: 1770–1772
19 Qi C H, Wu L A. A study of deterministic pilot allocation for sparse channel estimation in OFDM systems. Electron Lett, 2012, 16: 742–744
20 Sayeed A M, Behdad N. Continuous aperture phased MIMO: a new architecture for optimum line-of-sight links. In: Proceedings of 2011 IEEE International Symposium on Antennas and Propagation (APSURSI), Spokane, 2011. 293–296
21 Brady J, Behdad N, Sayeed A M. Beamspace MIMO for millimeter-wave communications: system architecture, modeling, analysis, and measurements. IEEE Trans Antennas Propagat, 2013, 61: 3814–3827
22 Hoydis J, Kobayashi M, Debbah M. Green small-cell networks. IEEE Veh Technol Mag, 2011, 6: 37–43
23 Zahir T, Arshad K, Nakata A, et al. Interference management in femtocells. IEEE Commun Surv Tutor, 2013, 15: 293–311
24 Zhang Q, Jin S, Huang Y M, et al. Uplink rate analysis of multicell massive MIMO systems in Ricean fading. In: Proceedings of Global Communications Conference, Austin, 2014. 3279–3284
25 Wang J, Jin S, Gao X, et al. Statistical eigenmode-based SDMA for two-user downlink. IEEE Trans Signal Process, 2012, 60: 5371–5383
26 Cao J, Wang D M, Li J M, et al. Uplink spectral efficiency analysis of multi-cell multi-user massive MIMO over correlated Ricean channel. 2017. https://arxiv.org/abs/1707.05915
27 Wang D M, Ji C, Gao X Q, et al. Uplink sum-rate analysis of multi-cell multi-user massive MIMO system. In: Proceedings of IEEE International Conference on Communications (ICC13), Budapest, 2013. 3997–4001